Complex band structure and the band alignment problem at the Si–high-*k* dielectric interface

A. A. Demkov,[1,*] L. R. C. Fonseca,[2] E. Verret,[1] J. Tomfohr,[3] and O. F. Sankey[3]
[1]*Freescale Semiconductor, Inc., Austin, Texas 78721, USA*
[2]*Freescale Semiconductores Brasil, Ltda., Jaguariúna, Brazil*
[3]*Arizona State University, Tempe, Arizona 85287-1504, USA*
(Received 26 October 2004; published 5 May 2005)

We investigate the use of the complex band structure of high-*k* gate dielectrics to estimate their charge neutrality levels, and compute band offsets to Si. A comparison is made with the available results obtained with direct electronic structure methods and experiment. It appears that charge neutrality levels thus obtained indeed provide a consistent picture for simple interfaces. However, the uncertainty in the conduction band position inherent in the local density approximation may render the theory inadequate for engineering support. Despite this limitation, linear rescaling of the charge neutrality levels based on the experimental band gaps for six oxides (SiO_2, Al_2O_3, *c*-HfO_2, *m*-HfO_2, La_2O_3, and $SrTiO_3$) has shown excellent agreement with experimental data.

DOI: 10.1103/PhysRevB.71.195306 PACS number(s): 73.40.Qv, 73.40.−c, 71.15.−m, 71.20.−b

I. INTRODUCTION

To insure continuous downscaling of CMOS technology the semiconductor industry must make a transition from the Si-SiO_2-poly-Si triad to a much more complex Si-dielectric-metal system.[1] The higher than silicon dioxide dielectric constant of the new gate dielectric will allow maintaining the gate capacitance and therefore the drain-source saturation current without reducing the oxide thickness. The integration of this new stack into the current CMOS flow is one of the most urgent tasks of today's electronics. The oxide's gate action, among other factors, depends on the barrier height at the oxide-semiconductor and oxide-metal interfaces. The band alignment is often estimated within the so-called metal-induced gap states (MIGS) model.[2,3] The MIGS model describes both the Bardeen and Schottky limits and interpolates between the two in a linear fashion, provided that electron affinities, charge neutralities, and the pinning factor are known. The theory was successfully used to describe the band discontinuity in hetero-junctions between covalent semiconductors. It is not obvious whether this approach should work for junctions between Si and high-*k* dielectrics. A consistent procedure to determine the charge neutrality level is also not clear. The reference potential method of van de Walle and Martin[4] produces reliable valence band offsets, and if the band gaps are known from experiment the conduction band offset can be inferred. However, these calculations are rather time consuming, and extremely sensitive to the exact structure of the interface. It would be very useful to have a simple phenomenological model to estimate the discontinuity. In this paper, following the recent work of Robertson,[5] we apply the simple MIGS model to the Si interface with SiO_2 (as a test) and four major high-*k* oxide families: simple metal, transition metal and lanthanide oxides, and epitaxial perovskites. We use the complex band structure to determine the charge neutrality level. We then compare these estimates of the band offset with those obtained *via* density functional theory (DFT) calculations. We find that the latter need to be performed with special care taken of the typical underestimation of the band gap, which may cause an unphysical band alignment and charge transfer.

II. THEORETICAL BACKGROUND

Recently, Robertson[5] used a variant of the MIGS model due to Tejedor, Flores, and Tersoff[6,7] (TFT) to predict conduction band offsets of a variety of novel dielectric materials. In this model the conduction band offset is given by

$$\phi = (\chi_a - \Phi_a) - (\chi_b - \Phi_b) + S(\Phi_a - \Phi_b). \tag{1}$$

Here χ is the electron affinity, Φ_i is the charge neutrality level of material *i* measured from the vacuum level, *S* is an empirical dielectric pinning parameter describing the screening by the interfacial states, and subscripts *a* and *b* refer to Si and dielectric, respectively. If $S=1$ the offset is given by a difference in electron affinities as was originally proposed by Schottky.[8] Alternatively, for $S=0$ we get the strong pinning or the Bardeen limit.[9] Bardeen suggested that the surface barrier is determined by the band bending caused by charging of the surface states,[10,11] and thus an intrinsic property of a material. The pinning parameter can be estimated by the empirical formula:[3]

$$S = \frac{1}{1 + 0.1(\varepsilon_\infty - 1)^2}, \tag{2}$$

where ε_∞ is the high frequency component of the dielectric constant. It is worth noting that a large value of ε_∞ would result in stronger pinning. The high frequency dielectric constant scales approximately as $1+(\hbar\omega_p/E_{PG})^2$, where ω_p is the plasma frequency that tracks the electron density $n(\omega_p = \sqrt{ne^2/\varepsilon_0 m})$, and E_{PG} is the so called Penn gap (a spectral weighted average of the band gap, typically 4 eV for semiconductors).[12] Thus a wide gap material would tend to have a smaller high frequency dielectric constant (the same conclusion can be achieved analyzing the Lindhard formula for the electronic susceptibility) and thus pin less. Electron affinities are typically well known experimentally. To estimate the position of the charge neutrality level Robertson used Tersoff's idea and associated it with the branch point of the complex band structure of the dielectric.[7] In a 1984 paper Tersoff also proposed a method to locate the branch point in the fundamental gap by calculating the zero of the Green's

function along a judiciously chosen crystallographic direction. Robertson uses a slightly different formula, which is appropriate for a tight-binding model since the energy spectrum has an upper bound (it has a finite number of bands); however in principle it is divergent.

We follow the same basic strategy; however, we find the branch point from the actual complex band structure. The analytical properties of Bloch functions and energies have been originally studied by Kohn and co-workers.[13] They considered the band energy $E_n(\vec{k})$ as a multivalued function $E(\vec{k})$ of a complex wave vector $\vec{k}=\vec{g}+i\vec{h}$. The usual band structure is then Re(E)-g cross section of the Riemann surface (the special case where h vanishes). Starting at the lower energy surface (e.g., the valence band) and going into the complex $\vec{k}$ plane around the branch point and back we end up on the next energy surface (e.g., the conduction band). Solutions of the Schrödinger equation for energies in the band gap thus have complex wave vectors, and are therefore spatially decaying. The wave function decays as $e^{-\vec{h}\cdot\vec{x}}$, and the charge density decays as $e^{-\beta x}$, where $\beta=2|\vec{h}|$. When we refer to a decay length, we will refer to the decay of the wave function; the decay length is then $1/h(=2/\beta)$. The character of the solution continuously changes from that of the lower energy band to the higher energy band, with the branch point serving as a point of crossover.[14] The physical connection between the wave vector at a branch point and the interfacial dipole was first made by Heine,[2] who used its inverse (the penetration depth of the evanescent gap state) to estimate the separation of the positive charge in the metal and negative charge in the surface states. Note that the complex band structure is a bulk property of a material, and thus can be calculated without a detailed interface model. To calculate the complex band structure we use the algorithm proposed by Boykin.[15] We use an LDA-DFT Hamiltonian implemented in the *ab initio* package SIESTA[16] with all the calculations performed using the minimal basis set (single-ζ–SZ) in order to simplify the analysis of the complex band structure. Because the band gap is underestimated, the branch point is uncertain. In the following we show that a simple scaling with respect to the experimental band gap value is sufficient to obtain a consistent picture.

III. RESULTS

A. Model verification: SiO_2

Si/SiO_2 is undoubtedly the most studied interface due to its ubiquitous use in the semiconductor devices.[17] To compare our method with well established experimental data we first consider this simple interface. We use crystalline β-cristobalite as a model for silicon dioxide which in practice is of course amorphous. The structure of β-cristobalite is given in Table I. The calculated band gap is 6.5 eV. Using the experimental value of 9.0 eV the complex band structure gives the rescaled charge neutrality level of β-cristobalite 5.1 eV above the valence band maximum (this places it 4.8 eV below the vacuum assuming an electron affinity χ of 0.9 eV). The charge neutrality level is found to be 3.7 eV above the valence band. We rescale this level according to the ratio of the computed and measured band gap to obtain 5.1 eV $[(9.0\ \text{eV}/6.5\ \text{eV})\times 3.7\ \text{eV}]$. The imaginary wave vector along the c axis of the tetragonal cell has a length of 0.67 Å^{-1} at the branch point, resulting in a very short decay length of the evanescent state of 1.5 Å.[18,19] This suggests a closely spaced double layer and a small potential rise attributed to its dipole (see Fig. 1). The electron affinity and charge neutrality level of Si with respect to vacuum are 4.0 and 4.9 eV, respectively.[5] The pinning parameter S of SiO_2 is 0.9 (almost ideal Schottky dielectric). The conduction band offset calculated using Eqs. (1) and (2) is 3.1 eV in rather good agreement with experiment and previous density functional calculations using the reference potential method.[20] Note that the large value of the pinning parameter manifests rather than explains that the barrier is close to the value predicted in the Schottky picture. The rapid decay of the evanescent state into the oxide is the physical reason, and it

TABLE I. Crystal structures of β-cristobalite, α-alumina, cubic and monoclinic hafnia, and lanthana used in the study. We list the chemical formula, space group, lattice constants, source of the information, and atomic positions in Wyckoff notations.

SiO_2, $Fd\bar{3}m$, $a=7.12$ Å, after Ref. 44
Si(1) 8a 0, 0, 0
O(1) 16c 0.125, 0.125, 0.125

Al_2O_3, $R\bar{3}c$, $a=4.759$ Å $c=12.991$ Å, after Ref. 45
Al(1) 12*c* 0 0 0.3520(3)
O(1) 18*e* 0.306(4) 0 0.25

c-HfO_2, $Fm\bar{3}m$, $a=5.111$ Å, after Ref. 46
Hf(1) 4*a* 0 0 0
O(1) 0 8*c* 0.25 0.25 0.25

m-HfO_2, P 1 21/*c* 1, $a=5.1156(5)$ Å, $b=5.1722(5)$ Å, $c=5.2948(5)$ Å, $\alpha=90.0°$, $\beta=99.18(8)°$, $\gamma=90.0°$, after Ref. 47
Hf(1) 4*e* 0.2759(5) 0.0412(5) 0.2078(5)
O(1) 4*e* 0.073(8) 0.346(8) 0.332(8)
O(2) 4*e* 0.446(8) 0.748(8) 0.488(8)

La_2O_3, $P\bar{3}m1$, $a=3.938$ Å, after Ref. 48
La (1) 2*d* 0.3333 0.6667 0.2467(2)
O (1) 2*d* 0.3333 0.6667 0.6470(2)
O (2) 1*a* 0.0 0.0 0.0

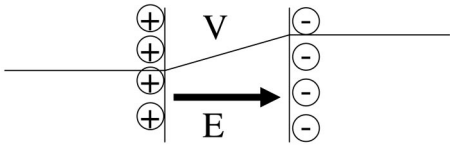

FIG. 1. The schematic of a double layer and a dipole potential at the interface. The potential rise V should be added to the discontinuity obtained from the Schottky rule $\Phi=\chi_i-\phi_m$. According to Heine (Ref. 2) the thickness of the double layer can be approximated by the decay length of the evanescent state in the band gap of the dielectric.

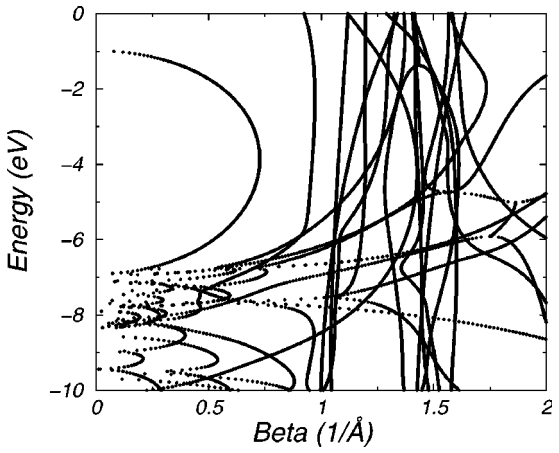

FIG. 2. The complex band structure of Al_2O_3 along the (001) direction. The valence band top is near −7 eV and the conduction band minimum is near −1 eV. The charge neutrality level is 3.1 eV above the band valence band top as calculated. The band gap is calculated to be 6.0 eV; therefore the rescaled value of the charge neutrality level is estimated to be 4.6 eV.

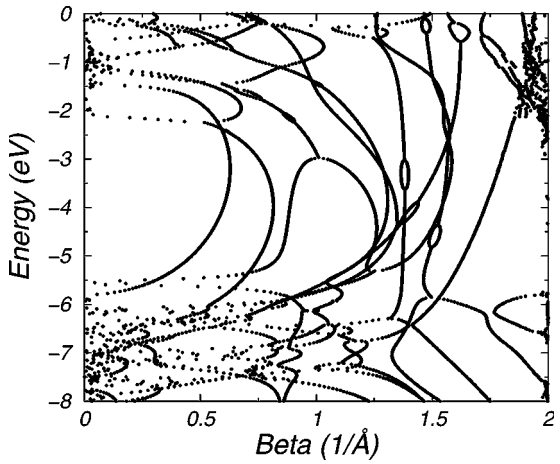

FIG. 3. The complex band structure of m-HfO_2 in the near gap region. The band gap lies in the range −2 eV to −5.5 eV. The charge neutrality level is 2.3 eV above the band valence band top as calculated. The band gap is calculated to be 3.5 eV; therefore the rescaled value of the charge neutrality level is estimated to be 3.8 eV.

stems from the large band gap and a low electron affinity: effectively SiO_2 behaves like a vacuum. The amount of charge in the double layer in Bardeen-Heine picture is governed by the initial difference between the charge neutrality level and the work function (for a true Schottky barrier) or between the charge neutrality levels in the case of a heterojunction.

B. Simple metal oxide: α-Al_2O_3

One of the major requirements for a successful gate oxide is a large band offset with Si (preferably over 1 eV) in both bands. To ensure the proper alignment it is best to start with a material that has a large band gap. Alumina with its band gap of 8.8 eV is second only to SiO_2 in that respect. We compute the complex band structure for α-Al_2O_3 and hope that the charge neutrality level and the evanescent state decay length thus obtained are representative of the more commonly used amorphous alumina. The crystal structure of α-Al_2O_3 is given in Table I. The complex band structure calculated along the (001) axis is shown in Fig. 2. Using the scaling argument we estimate the charge neutrality level to be 4.6 eV above the valence band top or 5.2 eV below the vacuum level (we follow Ref. 5 and use 1 eV for the electron affinity). At the charge neutrality level β [$\beta=2h$, where $h=\mathrm{Im}(k)$] is 0.71 which translates in the decay length of 2.8 Å. Note that the dipole layer at the alumina interface would thus be almost twice that of silica despite the similar band gaps.

C. Transition metal oxides: HfO_2

Hafnia emerges as the material of choice to substitute silica as a gate oxide. Films are typically grown by atomic layer deposition (ALD) and as deposited are amorphous. The postdeposition densification anneal results in film crystallization [the crystallization temperature of hafnia is only 350 °C (Ref. 21)], with tetragonal and monoclinic phase most commonly reported.[22] The structure of these two polymorphs is given in Table I. We have recently reported the complex band structure of the monoclinic form of hafnia.[19] Here we compare monoclinic and cubic polymorphs. In Fig. 3 we show the complex band structure calculated for monoclinic HfO_2. The charge neutrality level is 2.3 eV above the band valence band top. The band gap is calculated to be 3.5 eV, therefore a rescaled value of the charge neutrality level is estimated to be 3.8 eV using an experimental band gap for m-HfO_2 of 5.8 eV. Assuming the electron affinity of 2.5 eV,[5] the charge neutrality level is 4.5 eV with respect to vacuum. The length of the imaginary wave vector at the branch point along the (001) direction is ~ 0.3 Å^{-1}. Note that evanescent states penetrate much deeper in m-HfO_2 (about 3.3 Å) than in SiO_2 (about 1.5 Å). This together with a higher ε_∞ makes m-HfO_2 a strongly pinning material (indeed, $S=0.53$). The complex band is relatively flat in the vicinity of the branch point. This suggests a relative "insensitivity" of the result. The conduction band offset calculated using Eq. (1) is only 1.4 eV [Fig. 1(b)] while our previous DFT calculation using the reference potential method gives 1.8 eV (in this calculation a Si suboxide transition layer was included).[23] The situation may be salvaged if instead of Eq. (1) we assume n-type instead of intrinsic Si, thus Si behaves as a metal, and use the MIGS formula for a Schottky barrier:

$$\phi = S(\Phi_m - \Phi_b) + (\Phi_b - \chi). \tag{3}$$

Here Φ_m is the work function of Si. The resulting conduction offset is 1.8 eV in better agreement with DFT and experiment.[23]

In Fig. 4 we show the complex band structure of cubic hafnia. The charge neutrality level is 1.5 eV above the band valence band top as calculated, the band gap is calculated to be 3.0 eV, and therefore the rescaled value of the charge neutrality level is estimated to be 2.9 eV. At the charge neutrality level β [$\beta=2h$, where $h=\mathrm{Im}(k)$] is 0.42 which trans-

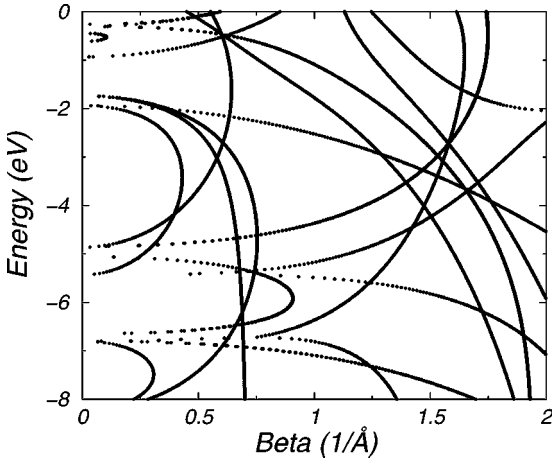

FIG. 4. The complex band structure of c-HfO_2 in the near gap region. The band gap lies between -5 eV and -2 eV. The charge neutrality level is 1.5 eV above the band valence band top as calculated. The band gap is calculated to be 3.0 eV; therefore the rescaled value of the charge neutrality level is estimated to be 2.9 eV.

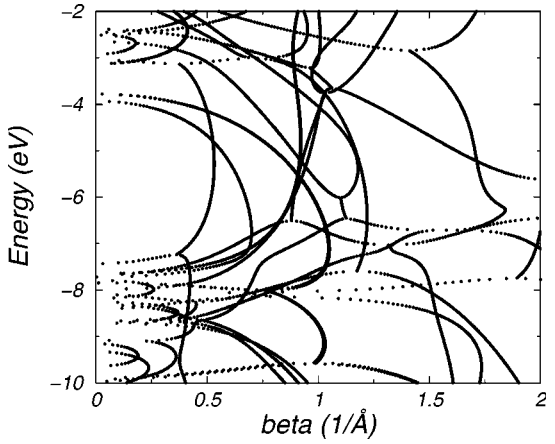

FIG. 5. (Color online) The complex band structure of La_2O_3 along the (001) direction. The charge neutrality level is 2.1 eV above the band valence band top as calculated. The band gap is calculated to be 3.5 eV; therefore the rescaled value of the charge neutrality level is estimated to be 3.6 eV.

lates in the decay length of 4.7 Å. This suggests a rather thick double layer, and potentially large dipolar correction to the Schottky rule.

It is worth mentioning that some of the experimental data used here is fairly old, and thus may not be reliable. Recent data for HfO_2 (Refs. 24 and 25) and ZrO_2 (Ref. 26) suggest slightly higher electron affinities. The band gap of HfO_2 varies with the synthesis and characterization technique; Nguyen *et al.* report 5.08 eV for Jet Vapor deposited films,[27] while Modrueanu *et al.* report values as high as 5.95 eV for MOCVD films,[28] the 5.8 eV value we use has been reported by Lim *et al.* for single crystal hafnia.[29] Density functional calculations for different interfacial models also vary by at least 0.5 eV.[30,31] The most significant result, however, is the mere fact that the charge neutrality level varies between different polymorphs significantly. This potentially spells troubles for CMOS applications. The typical grain size in the annealed ALD grown hafnia film is 60 Å, thus for 65 nm technology (65 nm gate length, and 0.2 μm gate width) there are approximately 300 grains under the gate. We will come back to this in Sec. III.

D. Lanthanide oxides: La_2O_3

Oxides of lanthanides such as lanthana,[32] ceria,[33] praseodymia,[34] and their alloys such as $LaAlO_3$ (Refs. 35 and 36) have recently been proposed as gate dielectrics. We consider hexagonal lanthana (La_2O_3) as a typical representative of this family. The structure of La_2O_3 is given in Table I. The complex band structure is shown in Fig. 5, which indicates that the charge neutrality level is 3.5 eV above the valence band top, or 4.5 eV below the vacuum level close to that of SiO_2 (this number should be taken with care since the accurate values of the band gap and electron affinity are not known—here we follow Ref. 5 and use 6 and 2 eV, respectively). We estimate β to be 0.56, which translates into the spatial decay of the evanescent state at the charge neutrality level of 3.6 Å. (See Table II.)

E. Epitaxial perovskites: $Si/SrTiO_3$

In contrast with amorphous and polycrystalline oxides discussed up to now, for MOS field effect devices with the gate length below 30 nm epitaxial oxides may offer certain advantages.[37] Recently epitaxial perovskite oxides on Si and Ge became a focus of attention.[38] We have also considered theoretically the interface between Si and $SrTiO_3$ (STO) using both the density of states and reference potential methods of analysis.[39] It is nevertheless instructive to discuss the MIGS theory predictions for this system. The electron affinities of Si and STO are 4.0 and 3.9 eV, respectively.[5] From the complex band structure of STO (not shown) the rescaled charge neutrality is 6.4 eV below vacuum. For Si it is 4.9 eV with respect to the vacuum level. Thus within the simple theory we expect a 1.6 eV conduction band offset in the

TABLE II. Experimental and calculated band gap, charge neutrality level (from the valence band maximum), and the evanescent state decay length for seven common oxides.

Oxide	Band gap (eV) Theory/ experiment	CNL (eV) scaled	CNL (eV) After Ref. 5	Decay length at CNL (Å)
SiO_2 (β cristobalite)	6.5/9.0	5.1		1.5
α-Al_2O_3	6.0/8.8	4.6	5.5	2.8
c-HfO_2	3.0/5.8	2.9		4.7
m-HfO_2	3.5/5.8	3.8	3.7	3.3
La_2O_3	3.5/6.0	3.5	2.4	3.6
$SrTiO_3$	1.8/3.3	1.3	2.6	2.0

Bardeen limit, and a 0.1 eV offset in the Schottky limit. The length of the imaginary wave vector at the branch point along the (001) direction is 0.5 $Å^{-1}$. It is interesting to note that despite a smaller band gap the evanescent states die off much faster in $SrTiO_3$ (within merely 2 Å) than in *m*-HfO_2 (3.3 Å). This anomalously rapid decay suggests a large value of the pinning parameter typical for the Schottky type alignment. Using the reference potential method as well as direct analysis of the site-projected density of states (PDOS), Zhang *et al*. find both a pure Schottky limit and a pinned Bardeen-like case depending on the interface structure.[39] They also estimated the *S* value of about 0.47 for the pinned interface [an empirical estimate gives 0.28 (Ref. 5)]. The Schottky case agrees well with experiment.[40]

IV. DISCUSSION

TM oxides at present are leading the race to succeed SiO_2 as a gate dielectric. To get a better understanding of the validity of Heine's theory for these materials we consider the electronic structure of a (111) surface slab of *t*-HfO_2 [plane-wave calculations are performed using CASTEP (Ref. 41)]. The full analysis of the structure and surface energetics will be reported separately.[42] The electronic band structure and density of states in the near gap region are shown in Fig. 6(a) (zero energy is set at the Fermi level). Note the occupied surface band approximately one electron volt wide located in the band gap region. The top of that surface band (and thus the Fermi level) is about 2.5 eV above the bulk top of the valence band, or approximately at the same energy as the predicted bulk charge neutrality level. In Fig. 6(b) we show the state at the -2.5 eV that is derived from oxygen *p* states as the top of the valence band should. The top of the surface band has a clear Hf character as can be seen in Fig. 6(c) [and is also indicated by the PDOS analysis (not shown)]. The states at the Fermi level thus appear to be derived from the dangling bonds on the metal. The density of these dangling bonds (Tamm-type surface states[10]) is much higher than that of the evanescent states (Shockley surface states[11]) and would therefore dominate the formation of the interface dipole. Surprisingly, they happened at approximately the same energy as the CNL determined from the complex band structure analysis.

To analyze the variation in the threshold voltage (the bias necessary to invert the channel and thus open the switch) due to the phase nonuniformity we perform device simulations providing estimates of threshold voltage shifts between grains of monoclinic and cubic HfO_2 polymorphs considering each as a simple capacitor. Mo is used as a metal gate, and the Mo/HfO_2 Schottky barrier is estimated using Eq. (3). We describe the metal-dielectric-semiconductor system with discrete grid points, and numerically solve Poisson's Eqs. (4),

$$\nabla \varepsilon \cdot \nabla \Psi = -q(p - n + N_d^+ - N_a^-), \tag{4}$$

where ε is the material permittivity, Ψ is the electrostatic potential, q is electronic charge, p and n are the concentration of holes and electrons, and N_d^+ and N_a^- are the concentration of ionized donors and acceptors, respectively. Knowing the potential distribution in the system permits calculation of the electric field (5):

$$\vec{E} = -\nabla \Psi. \tag{5}$$

From Gauss's law, the gate charge, Q_g, can be determined at a given gate voltage. The gate capacitance is calculated from the change in gate charge with respect to the change in gate voltage and is given by

$$C_g = \frac{\Delta Q_g}{\Delta V_g}. \tag{6}$$

Figure 7 shows the results of this calculation for a 1 μ^2 Mo/HfO_2 /Si capacitor with various substrate donor concentrations. Taking the derivative of gate capacitance with respect to gate voltage we define the threshold voltage, V_t, to be

$$V_t = \min\left(\frac{\Delta C_g}{\Delta V_g}\right). \tag{7}$$

The threshold voltage for monoclinic and cubic HfO_2 polymorphs are calculated for two cases where the Si/HfO_2 conduction band offset is given by Eq. (1) and Eq. (3). These results are shown in Fig. 8, where the change in threshold voltage of monoclinic HfO_2 referenced to cubic HfO_2, $\Delta V_{t_{C,M}}$, is shown for capacitors with low donor concentration and high donor concentration. As nominal device gate lengths continue to decrease with each technology generation, higher donor concentrations in the substrate for the PFETs are required to control short channel effects. At a donor concentration level 5×10^{18} cm^{-3} (where the Fermi level is closer to the valence band in silicon) $\Delta V_{t_{C,M}} = 0.04$ V. Considering decreases in threshold voltage are required to maintain performance as supply voltages are decreased, $\Delta V_{t_{C,M}} = 0.04$ becomes increasingly non-negligible as technology scaling continues. In addition, our analysis suggests that for fully depleted silicon on insulator (SOI) devices, where undoped channels (low doping limit in Fig. 8) are expected to be a likely device choice, the greater V_t variation would spell trouble for a midgap metal gate.

We would also like to comment on a potentially detrimental difficulty of the DFT calculations of the valence band offset for interfaces involving transition metal (TM) oxides. For the Si/HfO_2 interface we find a slightly *negative* Si/HfO_2 conduction band (CB) offset inferred from the calculations of the valence band offset using the reference potential method.[4] This problem appears to be a generic difficulty of the LDA Hamiltonian; the valence band offset (a ground state property) is well reproduced, and if the valence band offset is relatively large, the band gap "reduction" in the oxide region due to the LDA may result in qualitative errors. The problem is particularly severe for calculating Schottky barriers between TM oxides and small work function metals.

V. CONCLUSIONS

We have investigated the band alignment of novel gate dielectrics with Si using a simple model widely used in the literature. The essential ingredients of this model are the

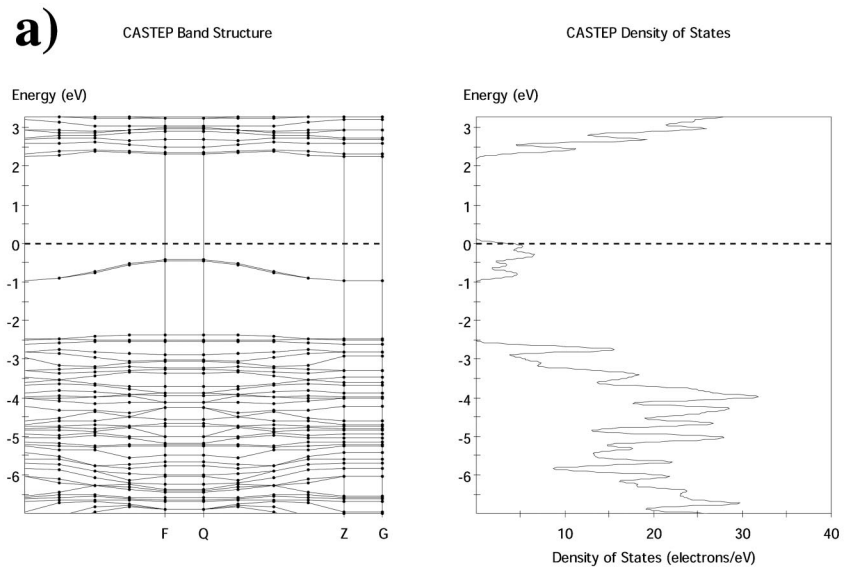

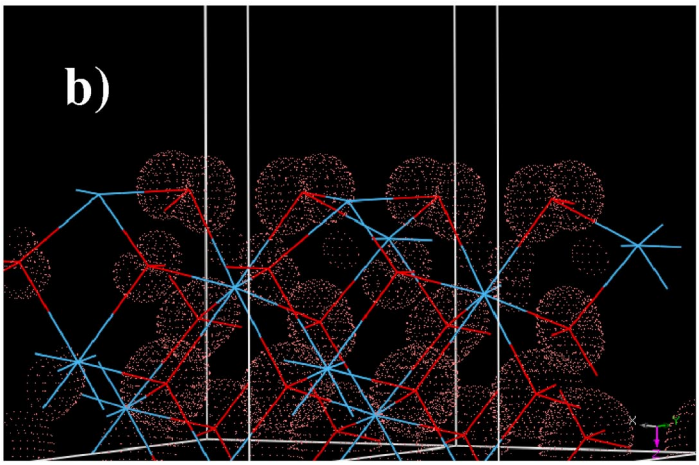

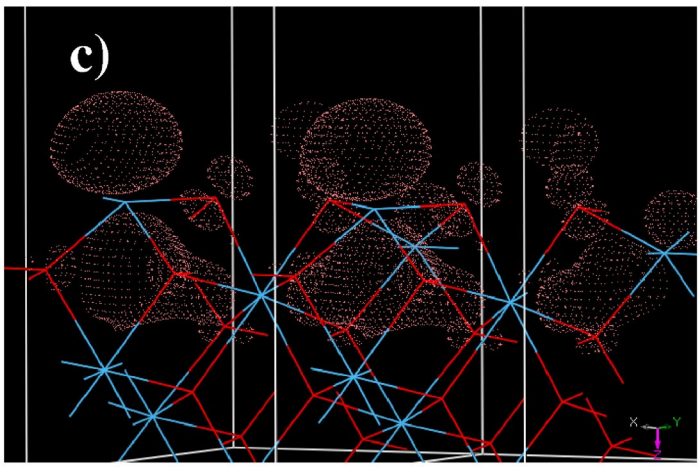

FIG. 6. (Color online) (a) The electronic structure of (111) *t*-HfO_2 surface slab. (b) The charge distribution at the top of the band at -2.5 eV is oxygen *p* state derived. (c) The state at the top of the occupied surface band at the Fermi level (set at zero energy) is Hf derived, its energy with respect to the valence band top approximately coinciding with that of the bulk charge neutrality level. The one electron volt wide surface band is separated from the bulk valence band top by a gap of about 1.5 eV.

electron affinity of both materials, the pinning strength of the dielectric, and the charge neutrality level of Si and the dielectric. The affinities are readily available from experiment, while the pinning strength can be approximated by a simple empirical rule. We have determined the charge neutrality level by performing complex band structure calculations for several oxide materials as originally proposed by Kohn. We find that though originally proposed to determine the offset at the semiconductor/semiconductor interface the model seems to work reasonably well for several complex systems,

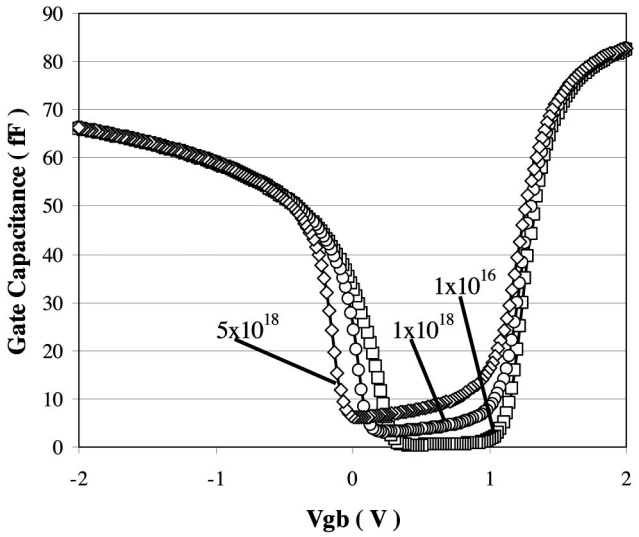

FIG. 7. A CV characteristic (gate capacitance versus gate voltage) of the Mo-*m*-HfO_2-Si structure for three doping levels.

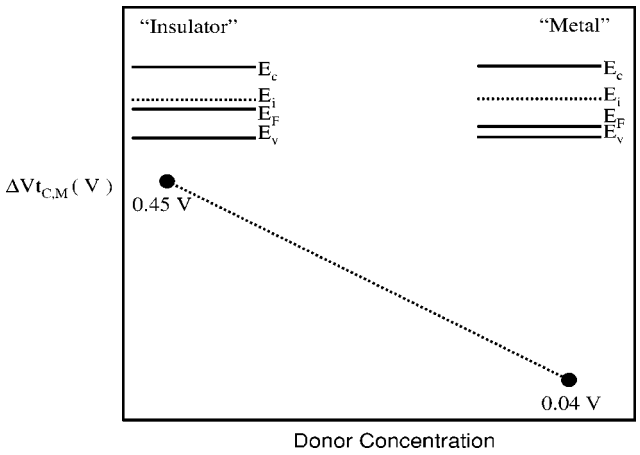

FIG. 8. Threshold voltage shift between monoclinic and cubic hafnia with silicon considered as "Insulator" [Eq. (1)] at low donor concentrations and "Metal" [Eq. (3)] at high donor concentrations.

at least where we are able to check by a direct calculation and comparison with experiment. Thus, the method appears to be useful in guiding experiment if the location of the CNL obtained from the complex band structure calculation is scaled by the experimental to theoretical band gaps ratio. On the other hand, the CNLs obtained from calculations using direct integration of the density of states[5] are in general not in good agreement with our results, except for the *m*-HfO_2 case. In particular, for alumina we find that Fermi level pinning should occur near the Si valence band edge, which is supported by the data of Hobbs *et al.*[43] while the approach used in Ref. 5 predicts pinning closer to the Si conduction band edge.

ACKNOWLEDGMENTS

It is our pleasure to thank Yong Liang, Rodney McKee, Sri Samavedam, David Gilmer, Phil Tobin, Scott Chambers, and John Robertson for many insightful discussions we had in the course of this work.

*Present address: Department of Physics, University of Texas at Austin, Austin, TX 78712. Email address: demkov@physics.utexas.edu

[1] 1999 International Technology Roadmap for Semiconductors, Semiconductor Industry Association, San Jose, 1999.
[2] V. Heine, Phys. Rev. **138**, A1689 (1965).
[3] W. Mönch, Surf. Sci. **300**, 928 (1994).
[4] C. G. Van de Walle and R. M. Martin, Phys. Rev. B **39**, 1871 (1989).
[5] J. Robertson and C. W. Chen, Appl. Phys. Lett. **74**, 1168 (1999); J. Robertson, J. Vac. Sci. Technol. B **18**, 1785 (2000).
[6] C. Tejedor, F. Flores, and E. Louis, J. Phys. C **10**, 2163 (1977).
[7] J. Tersoff, Phys. Rev. B **30**, 4874 (1984).
[8] W. Schottky, Z. Phys. **118**, 539 (1942).
[9] J. Bardeen, Phys. Rev. **71**, 717 (1947).
[10] Ig. Tamm, Phys. Z. Sowjetunion **1**, 733 (1932).
[11] W. Shockley, Phys. Rev. **56**, 317 (1939).
[12] P. Y. Yu and M. Cardona, *Fundamentals of Semiconductors* (Springer-Verlag, Berlin, 1996), p. 325.
[13] W. Kohn, Phys. Rev. **115**, 809 (1959); W. Kohn and C. Majumdar, Phys. Rev. **138**, A1617 (1965); W. Kohn and J. R. Onffroy, Phys. Rev. B **8**, 2485 (1973); J. J. Rehr and W. Kohn, Phys. Rev. B **9**, 1981 (1974); J. J. Rehr and W. Kohn, Phys. Rev. B **10**, 448 (1974).
[14] J. A. Appelbaum and D. R. Hamann, Phys. Rev. B **10**, 4973 (1974).
[15] T. Boykin, Phys. Rev. B **54**, 8107 (1996).
[16] D. Sanches-Portal, P. Ordejon, E. Artachio, and J. M. Soler, Int. J. Quantum Chem. **65**, 453 (1999).
[17] Y. J. Chabal, *Fundamental Aspects of Si Oxidation* (Springer-Verlag, Berlin, 2001).
[18] J. K. Tomfohr and O. F. Sankey, Phys. Status Solidi B **233**, 59 (2002).
[19] A. A. Demkov, L. R. C. Fonseca, J. K. Tomfohr, and O. F. Sankey, in *Fundamentals of Novel Oxide/Semiconductor Interfaces*, edited by C. R. Abernathy, E. Gusev, D. Schlom, and S. Stemmer, MRS Symposia Proceedings No. 786 (Materials Research Society, Pittsburgh, 2004), p. 29.
[20] A. A. Demkov and O. F. Sankey, Phys. Rev. Lett. **83**, 2038 (1999).
[21] S. V. Ushakov, A. Navrotsky, Y. Yang, S. Stemmer, K. Kukli, M. Ritala, M. A. Leskelä, P. Fejes, A. A. Demkov, C. Wang, B.-Y. Nguyen, D. Triyoso, and P. Tobin, Phys. Status Solidi B **241**, 2268 (2004).
[22] A. A. Demkov, D. Triyoso, P. Fejes, and R. Gregory (unpublished).
[23] L. Fonseca, A. A. Demkov, and A. Knizhnik, Phys. Status Solidi B **239**, 48 (2003).
[24] T. E. Cook, Jr., C. C. Fulton, W. J. Mecouch, R. F. Davis, G. Lucovsky, and R. J. Nemanich, J. Appl. Phys. **94**, 7155 (2003).

[25] S. Sayan, E. Garfunkel, and S. Suzer, Appl. Phys. Lett. **80**, 2135 (2002); S. Sayan, T. Emge, E. Garfunkel, X. Zhao, L. Wielunski, R. A. Bartynski, D. Vanderbilt, J. S. Suehle, S. Suzer, and M. Banaszak-Holl, J. Appl. Phys. **96**, 7485 (2004).

[26] S. Sayan, T. Emge, E. Garfunkel, M. Croft, X. Zhao, D. Vanderbilt. N. V. Nguyen, J. Ehrstein, I. Levin, E. P. Gusev, H. Kim, and P. J. McIntyre (unpublished).

[27] N. V. Nguyen, J.-P. Han, J. Y. Kim, E. Wilcox, Y. J. Cho, W. Zhu, Z. Luo, and T. P. Ma, in *Characterization and Metrology for ULSI Technology*, International Conference, edited by D. G. Seiler, A. C. Dielbold, T. J. Shaffner, R. McDonald, S. Zollner, R. P. Khosla, and E. M. Secula (AIP Press, Melville, NY, 2003), p. 181.

[28] M. Modreanu, P. K. Hurley, B. J. O'Sullivan, B. O'Looney, J. P. Senateur, H. Rousell, F. Rousell, M. Audier, C. Dubourdieu, I. W. Boyd, Q. Fang, T. L. Leedham, S. Rushworth, A. C. Jones, H. Davies, and C. Jimenez, Proc. SPIE **4876**, 1236 (2002).

[29] S.-G. Lim, S. Kriventsov, T. N. Jackson, J. H. Haeni, G. G. Schlom, A. M. Balbashov, R. Uecker, P. Reiche, J. L. Freeouf, and G. Lucovsky, J. Appl. Phys. **91**, 4500 (2002).

[30] L. Fonseca and A. Knizhnik (unpublished).

[31] R. Puthenkovilakam and J. Chang, Appl. Phys. Lett. **84**, 1353 (2004).

[32] Y. T. Hou, M. F. Li, H. Y. Yu, and K. L. Kwong, *Proceedings of the 2003 Symposia on VLSI Technology and Circuits* (VLSI, Kyoto, 2003).

[33] W. He, S. Schuetz, R. Solanki, J. Belot, and J. McAndrew, Electrochem. Solid-State Lett. **7**, G131 (2004).

[34] T. M. Pa, C. H. Chien, T. F. Lei, T. S. Chao, and T. Y. Huang, Electrochem. Solid-State Lett. **4**, F15 (2004).

[35] H. J. Osten, J. P. Liu, P. Gaworzewski, E. Bugiel, and P. Zaumseil, IEDM 2001.

[36] L. Yan, H. B. Lu, G. T. Tan, F. Chen Y. L. Zhou, G. Z. Yang, W. Liu, and Z. H. Chen, Appl. Phys. A: Mater. Sci. Process. **77**, 721 (2003).

[37] R. Droopad, K. Eisenbeiser, and A. A. Demkov, in *Alternative Gate Dielectrics*, edited by H. Huff and D. Gilmer (Springer-Verlag, Berlin, 2004).

[38] R. A. McKee, F. J. Walker, and M. F. Chisholm, Phys. Rev. Lett. **81**, 3014 (1998); R. A. McKee, F. J. Walker, and M. F. Chisholm, Science **293**, 461 (2001).

[39] X. Zhang, A. A. Demkov, Hao Li, X. Hu, Yi Wei, and J. Kulik, Phys. Rev. B **68**, 125323 (2003).

[40] S. Chambers, Y. Liang, Z. Yu, R. Droopad, J. Ramdani, and K. Eisenbeiser, Appl. Phys. Lett. **77**, 1662 (2000).

[41] V. Milman, B. Winkler, J. A. White, C. J. Pickard, M. C. Payne, E. V. Akhmatskaya, and R. H. Nobes, Int. J. Quantum Chem. **77**, 895 (2000).

[42] A. A. Demkov (unpublished).

[43] C. C. Hobbs, L. R. C. Fonseca, A. Knizhnik, V. Dhandapani, S. B. Samavedam, W. J. Taylor, J. M. Grant, L. G. Dip, D. H. Triyoso, R. I. Hegde, D. C. Gilmer, R. Garcia, D. Roan, M. L. Lovejoy, R. S. Rai, E. A. Hebert, Hsing-Huang Tseng, S. G. H. Anderson, B. E. White, and P. J. Tobin, IEEE Trans. Electron Devices **51**, 971 (2004); **51**, 978 (2004) (part 1 and part 2).

[44] R. W. G. Wyckoff, Z. Kristallogr. **62**, 189 (1925).

[45] R. E. Newnham and Y. M. de Haan, Z. Kristallogr. **117**, 235 (1962).

[46] L. Passerini, Gazz. Chim. Ital. **60**, 762 (1930).

[47] R. Ruh and P. W. R. Corfield, J. Am. Ceram. Soc. **53**, 126 (1970).

[48] P. Aldebert and J. P. Traverse, Trans. J. Br. Ceram. Soc. **83**, 92 (1984).